JVI Journals.ASM.org

Viral Reprogramming of the Daxx Histone H3.3 Chaperone during Early Epstein-Barr Virus Infection

Kevin Tsai,[a,b] Lilian Chan,[a] Rebecca Gibeault,[c] Kristen Conn,[c] Jayaraju Dheekollu,[a] John Domsic,[a,b] Ronen Marmorstein,[a,b] Luis M. Schang,[c] Paul M. Lieberman[a]

The Wistar Institute, Philadelphia, Pennsylvania, USA[a]; Perelman School of Medicine, The University of Pennsylvania, Philadelphia, Pennsylvania, USA[b]; Department of Biochemistry, University of Alberta, Edmonton, Alberta, Canada[c]

ABSTRACT

Host chromatin assembly can function as a barrier to viral infection. Epstein-Barr virus (EBV) establishes latent infection as chromatin-assembled episomes in which all but a few viral genes are transcriptionally silent. The factors that control chromatin assembly and guide transcription regulation during the establishment of latency are not well understood. Here, we demonstrate that the EBV tegument protein BNRF1 binds the histone H3.3 chaperone Daxx to modulate histone mobility and chromatin assembly on the EBV genome during the early stages of primary infection. We demonstrate that BNRF1 substitutes for the repressive cochaperone ATRX to form a ternary complex of BNRF1-Daxx-H3.3-H4, using coimmunoprecipitation and size-exclusion chromatography with highly purified components. FRAP (fluorescence recovery after photobleaching) assays were used to demonstrate that BNRF1 promotes global mobilization of cellular histone H3.3. Mutation of putative nucleotide binding motifs on BNRF1 attenuates the displacement of ATRX from Daxx. We also show by immunofluorescence combined with fluorescence *in situ* hybridization that BNRF1 is important for the dissociation of ATRX and Daxx from nuclear bodies during *de novo* infection of primary B lymphocytes. Virion-delivered BNRF1 suppresses Daxx-ATRX-mediated H3.3 loading on viral chromatin as measured by chromatin immunoprecipitation assays and enhances viral gene expression during early infection. We propose that EBV tegument protein BNRF1 replaces ATRX to reprogram Daxx-mediated H3.3 loading, in turn generating chromatin suitable for latent gene expression.

IMPORTANCE

Epstein-Barr Virus (EBV) is a human herpesvirus that efficiently establishes latent infection in primary B lymphocytes. Cellular chromatin assembly plays an important role in regulating the establishment of EBV latency. We show that the EBV tegument protein BNRF1 functions to regulate chromatin assembly on the viral genome during early infection. BNRF1 alters the host cellular chromatin assembly to prevent antiviral repressive chromatin and establish chromatin structure permissive for viral gene expression and the establishment of latent infection.

Cellular chromatin assembly is a highly regulated process required for the control of programmed gene expression and genome stability (reviewed in reference 1). DNA viruses that enter the nucleus are subject to chromatin assembly and chromatin structures that regulate viral gene expression and replication. Cell-mediated chromatin assembly may also function to resist viral infection (2, 3). To ensure the expression of viral genes essential for productive infections, viruses encode numerous factors that counteract cellular antiviral resistances such at chromatin-mediated silencing (4, 5). The mechanisms of viral modulation of chromatin assembly are not completely understood and may be different for each virus and their respective infection strategies.

Almost all viruses that enter the nuclear compartment interact with prominent nuclear structures referred to as the promyelocytic leukemia nuclear bodies (PML-NBs; also called ND10) (4, 6, 7). PML-NBs are interferon-inducible structures that frequently form adjacent to viral genomes that just entered the nucleus. The PML protein forms a major structural component of the PML-NBs that typically also include Sp100, Daxx, and ATRX (7). They are disrupted by a variety of virus-encoded proteins, strongly suggesting that PML-NBs are involved in antiviral resistance (8). Most virus-targeted PML-NB components, such as Daxx, ATRX, and Sp100, are involved in chromatin regulation and gene repression. Sp100 represses gene expression from foreign DNA (9, 10). Daxx is a transcription corepressor that interacts with cellular transcription factors (11–15) and heterochromatin associated factors such as histone deacetylases and DNA methyltransferase I (15–18). ATRX, a protein with a SWI/SNF-like ATPase motif (19), is associated with the establishment of heterochromatin (20, 21). More recently, Daxx has been found to form with ATRX a chromatin remodeling complex that acts as a histone chaperone of the histone variant H3.3 (22, 23). Histone H3.3 is loaded on chromatin in a DNA replication-independent manner, while H3.1 is typically assembled by CAF-I during DNA replication (24). H3.3 can be loaded onto transcriptionally active regions by the histone chaperone HIRA (25). In contrast, Daxx and ATRX have been found to load histone H3.3 onto pericentric and subtelomeric chromatin (26) and are associated with the silencing of transcription from these regions. Furthermore, Sp100, Daxx, and ATRX

Received 2 July 2014 **Accepted** 26 September 2014
Published ahead of print 1 October 2014
Editor: R. M. Longnecker
Address correspondence to Paul M. Lieberman, lieberman@wistar.org.

doi:10.1128/JVI.01895-14

have been reported to orchestrate host-induced repression of viral gene expression shortly after viral entry. PML and Sp100 represses herpes simplex virus 1 (HSV-1) gene expression (27), whereas Daxx and ATRX have been reported to confer heterochromatic markers on viral genomes of both human cytomegalovirus (HCMV) and adenovirus type 5 (Ad5) (28, 29).

Epstein-Barr virus (EBV) is a human gammaherpesvirus associated with several malignancies, including Burkitt's lymphoma and nasopharyngeal carcinoma (reviewed in reference 30). EBV is notable for its propensity to establish latent infections in human B lymphocytes where the viral genome persists as a chromatinized episome expressing only a few viral genes (reviewed in references 31 and 32). It is thought that viral chromatin assembly during primary infection is an important regulator of early viral gene expression and the establishment of successful latent infection (33). The establishment of EBV latency requires chromatin control in order to limit viral gene expression to a small number of latency-associated genes. However, little is known of how this latent infection is established upon the early stages of primary infection, which has been referred to as the pre-latent phase (34). Viral chromatin assembly and epigenetic programming are thought to initiate during this prelatency phase.

The EBV-encoded tegument protein BNRF1 is among the most abundant viral proteins brought into host cells by the infecting virions (35). It is a member of a highly conserved family found in all gammaherpesviruses, including KSHV ORF75 (36), MHV68 ORF75c (37), and HVS ORF3 (38). Each family member contain sequence homology to the cellular purine biosynthesis enzyme phosphoribosylformylglycineamide amidotransferase (FGARAT). However, no enzymatic activity of these viral FGARAT-homology proteins have been reported. All studied homologs have been reported to disrupt different components of PML-NB. EBV BNRF1 was previously reported to be important for EBV early infection (39). We recently found that BNRF1 dissociates ATRX from Daxx and promotes viral gene expression during primary infection (40). Here, we investigate whether BNRF1 modifies the histone H3.3 chaperone function of Daxx. We show that while displacing ATRX from Daxx, BNRF1 forms a stable complex with the histone chaperone complex consisting of Daxx and histone variant H3.3 and H4, displacing ATRX. Consequently, BNRF1 increases histone H3.3 dynamics in the nucleus. During the prelatency phase of EBV infection, the tegument-delivered BNRF1 promotes viral gene expression, increases the presence of transcriptionally active histone marker H3K4 trimethylation (H3K4me3), and prevents the deposition of histone H3.3, Daxx, and ATRX on latency control elements. We propose that BNRF1 replaces the chaperone-guiding function of ATRX to allow productive chromatin assembly on EBV genomes during primary infection of B lymphocytes, in turn allowing the expression of viral latent genes and the establishment of latent infection.

MATERIALS AND METHODS

Ethics statement. Human donor blood was collected from anonymous adult donors by the Wistar Institute phlebotomy lab and approved by the Wistar Institute Institutional Review Board. Written informed consent was provided by study participants.

Cells. 293T cells were grown in Dulbecco modified Eagle medium (DMEM; Mediatech Corning) with 11% fetal bovine serum (FBS; Atlanta Biologicals), 20 mM GlutaMAX (Gibco), 100 U/ml penicillin, and 100 μl/ml streptomycin. Mutu I and EBV-negative Akata cells were grown in RPMI 1640 medium (Mediatech Corning) supplemented with 11% FBS. African green monkey (Vero) cells were maintained in DMEM with 5% FBS. All cells were grown in a 5% CO_2 incubator at 37°C. 293/EBV-wt and 293/ΔBNRF1 cells were grown in DMEM with 10% FBS and 100 μg/ml hygromycin to ensure bacmid retention. Primary B cells were isolated from donated human blood by density gradient centrifugation with Ficoll-Paque Plus (GE Healthcare), followed by use of a Dynabeads Untouched Human B cell isolation kit (Invitrogen) or EasySep Human B cell enrichment kit (Stemcell Technologies). Mutu I and EBV-negative Akata cells are EBV-positive and -negative (respectively) Burkitt's lymphoma cell lines.

Plasmids. pcDNA3-HA-Daxx was a generous gift from Hsiu-Ming Shih (41). FLAG-BNRF1 expression vector was constructed as described previously (40). Daxx and BNRF1-FGARAT domain deletions were produced by site-directed mutagenesis (40). The Daxx interaction domain (DID; amino acids [aa] 360 to 600 [360-600aa]) of BNRF1 was cloned into the NotI and SalI sites of a pRSF-GST vector. pRUTH5-Daxx-HBD (183-398aa) and the bacterial expression vectors of H3.3 and H4 were kindly provided by Dinshaw Patel (42). For the fluorescence recovery after photobleaching (FRAP) assays, the BNRF1 (wild type [WT] and mutants) coding sequence was cloned into the HindIII-SalI sites of the pCMV-mCherry-C3 expression vector. The plasmids encoding EGFP-H2B (43) and EGFP-H3.3 (a generous gift from John Th'ng, Northern Ontario School of Medicine) were constructed as described previously (44). All plasmid maps and cloning details are available upon request.

Antibodies. Mouse anti-FLAG (F1804), rabbit anti-FLAG (F7425), anti-Daxx (F7810), anti-β-actin peroxidase antibody (A3854) were purchased from Sigma-Aldrich. Rabbit anti-ATRX (H-300, sc-15408) and nonspecific rabbit IgG (sc-2027) were purchased from Santa Cruz Biotechnology. Mouse anti-HA tag (6E2) and Rabbit anti-GST (91G1) antibodies were purchased from Cell Signaling Technology. Rabbit anti-histones H3.3 (catalog no. 09-838), pan-H3 (catalog no. 07-690), and H3K4me3 (catalog no. 07-473) were purchased from Millipore. Rabbit serum anti-H3K9me3 (39161) were from Active Motif. Rabbit anti-PARP1 antibody (ALX-210-895-R100) was purchased from Enzo Life Sciences. Rabbit anti-BNRF1 was raised against the 1296-1318aa fragment of BNRF1, custom produced by YenZym Antibodies, LLC.

Virus production. Virus was produced using bacmids of the EBV genome. 293/EBV-wt and 293/ΔBNRF1 cells (gifts from H. J. Delecluse) are 293HEK cells stably transfected with the EBV bacmid; the former contains WT B95-8 viral genome (45), and the latter has the BNRF1 gene deleted (39). siCtrl and siBNRF1 virus was induced by cotransfecting 293/EBV-wt cells in 60-mm dishes with expression plasmids of 0.75 μg of BALF4, 1.5 μg of BZLF1, 5 μl of 40 μM small interfering RNA (siRNA), and 5 μl per plate of DharmaFECT Duo reagent (Thermo Scientific) according to the manufacturer's instructions. All siRNAs were purchased from Dharmacon Thermo Scientific. siCtrl is ON-TARGETplus Nontargeting siRNA 1 D-001810-01-05. BNRF1-targeting siRNAs are custom designed with Dharmacon's online design tool, including one with a target sequence inside the open reading frame (sequence CGAGCAAGGUC CAGAUCAAUU) and one targeting the 3′-untranslated sequence (sequence CAAUAAACCCAAUGUGCAAUU). BNRF1 null virus from 293/ΔBNRF1 cells was generated as previously mentioned (40). Mutu virus was generated by culturing Mutu I cells at a concentration of 0.5 million cells/ml in 50 to 60 ml of RPMI with 50% spent medium and 50% fresh medium. The culture medium was supplemented with 1 mM sodium butyrate and 12-*O*-tetradecanoylphorbol-13-acetate (TPA) at 20 μg/ml to induce viral production. All virus-containing supernatants were collected 5 to 7 days postinduction, centrifuged at 1,500 rpm for 10 min, and filtered through 0.45-μm-pore-size filters to remove contaminating cells. Virus were concentrated by ultracentrifugation at 10,000 × *g* 2 h at 4°C. Quantitative PCR (qPCR) quantification of the virus titer was performed as previously described (40).

Immunoprecipitation assays. For Daxx-histone interactions, IP was performed as described previously (42) with minor modifications. After NaCl was added to extract nuclear proteins, the samples were sonicated for 30 s on and 1 min off for 5 min to clear the genomic DNA and then precleared for 2 h with 50 μl (per IP) of 50% slurry protein A-beads.

Lysates were centrifuged for 2 min at 3,000 rpm at 4°C to remove beads and debris. Then, 4 μg of antibodies or 25 μl of FLAG-beads (Sigma A2220)/IP was incubated overnight. For the IP of native BNRF1 from Mutu I virus-infected primary B cells, cells were collected 2 days postinfection and subjected to IP as described previously (40), with the exception of using protein A-beads precoupled with nonspecific rabbit IgG or rabbit anti-BNRF1 antibody. Coupling of antibodies to beads was done with dimethylpimelimidate as described previously (46). All other IP methods were performed as described previously (40).

GST pulldown assays. Glutathione *S*-transferase (GST)-BNRF1-DID protein was produced in *Escherichia coli*, which was subsequently purified with glutathione-Sepharose 4B (Amersham) and dialyzed into binding buffer (150 mM KCl, 0.01 M Tris-HCl [pH 7.5], 10% glycerol, 0.5 mM EDTA, 1 mM dithiothreitol [DTT], 1 mM phenylmethylsulfonyl fluoride [PMSF]). Dignam nuclear extracts were prepared from 9×10^6 Mutu I cells (47). For the pulldown assay, GST-BNRF1-DID was prebound to glutathione beads, incubated with Dignam nuclear extracts overnight 4°C, and then washed four times in TEK150 buffer (20 mM Tris [pH 7.5], 150 mM KCl, 0.1 mM EDTA, 1 mM DTT, 1 mM PMSF). Proteins were eluted by boiling samples directly in Laemmli buffer, followed by Western blot analysis.

Size-exclusion chromatography. GST-BNRF1-DID 360-600aa, His-tagged Daxx 183-398aa, His-tagged H3.3, and His-tagged H4 were expressed in *E. coli*. GST-BNRF1 360-600aa was purified as a soluble protein in 0.5 M NaCl, 20 mM HEPES, and 0.1 mM TCEP [*tris*(2-carboxyethyl)phosphine], pH 8.0, using glutathione-Sepharose. The tag was removed with tobacco etch virus (TEV) protease, and the BNRF1 was purified by ion exchange, followed by gel filtration chromatography using a Superdex S75 column. Daxx, H3.3, and H4 were purified from inclusion bodies as described previously (48). Purified Daxx, H3.3, and H4 (or only H3.3 and H4) were mixed at an equimolar ratio in 8 M urea, dialyzed against 3.5 M urea, and then extensively dialyzed against 1.0 M NaCl–20 mM HEPES–0.1 mM TCEP (pH 7.5). We were unable to purify Daxx alone as a soluble protein. The complexes were then purified by ion-exchange chromatography and gel filtration. Purified BNRF1 was then mixed with Daxx/H3.3/H4 or H3.3/H4 at an equimolar ratio in 1.0 M NaCl–20 mM HEPES–0.1 mM TCEP (pH 7.5) and loaded onto a Superdex 200 column equilibrated with the same buffer.

Analysis of H3.3 dynamics by FRAP. Cells were transfected as described previously (49), with the following modifications: 2.2×10^5 to 2.4×10^5 Vero cells were transfected with 6 μl of Lipofectamine 2000 (Invitrogen), 6 to 8 μg of green fluorescent protein (GFP)-histone plasmids, and 5 μg of Cherry-BNRF1 (WT or d26 or dATPase mutants) or Cherry-C3 plasmids. After 6.5 h of incubation with the transfection mixture, 1 ml of DMEM prewarmed to 37°C was added to the cells. Cells were seeded onto coverslips the following day and analyzed at least 4 h later. The bulk of GFP-histone H3.3 is incorporated into chromatin at this time (44). Histone mobilization was evaluated by FRAP as described previously (49). Fluorescence within the photobleached region was normalized to total nuclear fluorescence and expressed relative to the normalized fluorescence of the same region before photobleaching to account for differences between GFP-H3.3 expression levels between cells. The relative free pool and slow exchange rate were obtained by expressing the relative fluorescence intensity of cells expressing detectable levels of WT, d26, or dATPase red fluorescent protein (RFP)-BNRF1 or free RFP as a ratio to that of cells not expressing detectable levels on each coverslip. More than 15 cells per treatment from at least three independent experiments were quantitated. Statistical significance was tested using one-tailed Student *t* test.

Primary infection for testing prelatency stage events. Primary B lymphocytes were mixed with concentrated EBV at a ratio of 100 viral DNA copies per cell (multiplicity of infection [MOI] of 100) for bacmid-produced virus or an MOI of 30 for Mutu strain virus. The B cell-virus mixture was seeded at 0.8 million cells in 0.5 ml virus per well in 48-well plates, spun down at 1,200 rpm for 5min, and then incubated at 37°C for 3 to 4 h. Half of the viral media was then replaced with fresh RPMI medium. Infected cells were harvested at 72 h postinfection (hpi; or the specified time points for time course studies) and washed with phosphate-buffered saline (PBS) to remove potentially contaminating loosely attached virions.

ChIP. Chromatin immunoprecipitation (ChIP) was performed as previously described (50), with minor modifications (delineated in reference 51). Specifically, cells were cross-linked with 2 mM EGS (Thermo Pierce, catalog no. 21565) in PBS for 45 min, followed by 1% formaldehyde for 20 min, and then quenched with 0.125 M glycine. Pulled-down DNA fragments were analyzed by real-time PCR (data not shown).

IF-FISH. EBV-infected primary B cells were harvested, washed in PBS, and mounted onto slides by cytospin (Shandon Cytospin 3; Thermo Fisher) at 1,000 rpm for 5 min. To visualize Daxx and ATRX, indirect immunofluorescence (IF) was performed as previously described (52). In preparation for subsequent fluorescent *in situ* hybridization (FISH), slides were fixed again in 1× PBS with 3% paraformaldehyde for 10 min, incubated in 0.1 M HCl–0.7% Triton in 1× PBS for 10 min on ice—with 2× SSC (1× SSC is 0.15 M NaCl plus 0.015 M sodium citrate) washes before and after, and then air dried. FISH detection of viral DNA was carried out as previously described (53). Samples were photographed with a Nikon E600 microscope using a 60× objective lens in conjunction with Image-Pro 7.0 software.

RT-qPCR assay. Reverse transcription (RT)-qPCR assay of viral gene expression was performed as previously described (40; unpublished data).

shRNA-mediated knockdown of Daxx and ATRX. EBV-negative Akata cells were infected with shRNA-carrying lentivirus and then selected with puromycin as described previously (40). All shRNA lentivirus constructs are gifts from Roger Everett.

RESULTS

BNRF1 interacts with the histone binding domain of Daxx. Daxx and ATRX form a histone H3.3 chaperone complex (22), the structure of which was recently published (42). We first sought to locate the site on Daxx that BNRF1 interacts with, specifically seeking to determine whether this interaction site overlaps with the Daxx histone-binding domain (HBD). Several mutations were introduced into a hemagglutinin (HA)-tagged Daxx expression construct, including deletions of sequences amino terminal (ΔN), within (ΔHBD), and carboxy terminal (ΔC) to the HBD at 178 to 389 aa (42). We also made an HBD-only construct by deleting N- and C-terminal flanking regions (Fig. 1A). HA-Daxx constructs were cotransfected with FLAG-tagged BNRF1 into 293T cells, and cell lysates were subject to immunoprecipitation (IP) with FLAG-affinity beads. FLAG-BNRF1 copurified with wild-type (WT), ΔN, ΔC, and HBD-alone Daxx constructs but not ΔHBD (Fig. 1B). No Daxx proteins were immunoprecipitated in control transfections lacking FLAG-BNRF1 (data not shown). These results indicate that BNRF1 interacts selectively with the Daxx HBD domain.

BNRF1 forms a complex with Daxx and the histone H3.3/H4 tetramer. The observation that BNRF1 interacts with the HBD of Daxx raised the possibility that BNRF1 may interfere with H3.3 loading by steric hindrance of Daxx-histone interaction. To test this possibility, we transfected 293T cells with HA-Daxx, with or without GFP-BNRF1, and FLAG-tagged histone variant H3.1 or H3.3. Transfected cell lysates were subject to IP assay with anti-Daxx or anti-FLAG (histone) (Fig. 1C). As expected, anti-Daxx pulled down more FLAG-H3.3 than FLAG-H3.1. Daxx also pulled down BNRF1 as previously reported (40). Interestingly, the interaction was enhanced in the presence of FLAG-H3.3. Importantly, FLAG-IP of histone H3.3 pulled down both Daxx and BNRF1. The BNRF1-Daxx-H3.3 interaction was selective for H3.3 since the FLAG pull down of H3.1 yielded 3-fold less Daxx and BNRF1 than FLAG-H3.3 pull downs (Fig. 1C, compare lanes 8 and 16 to lanes 2 and 10). This is consistent with published studies showing

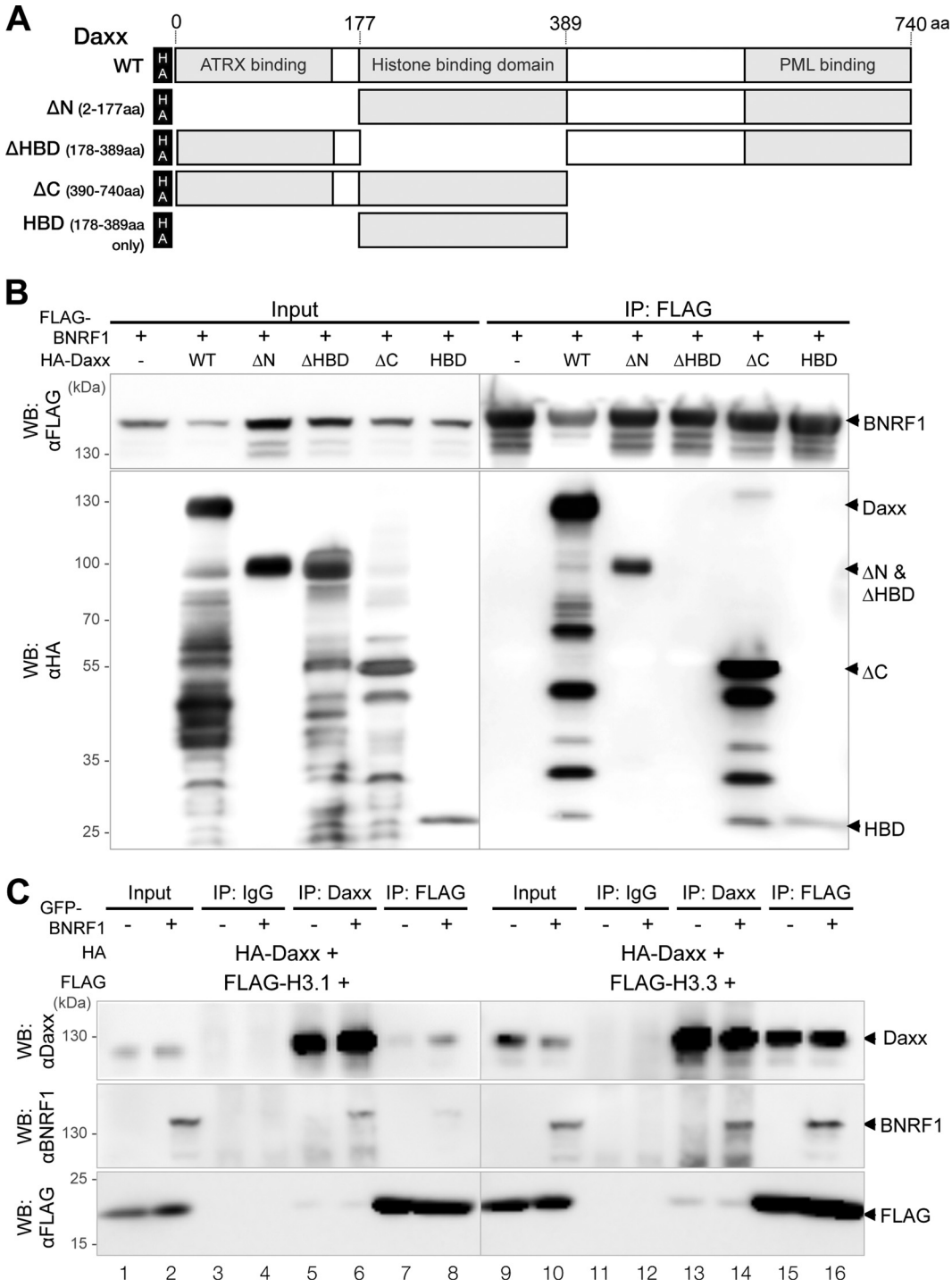

FIG 1 BNRF1 binds Daxx on its histone-binding domain (HBD) and copurifies with histone H3.3. (A) Diagram of HA-Daxx deletion constructs with functional domains indicated. (B) Immunoprecipitation (IP) assay of FLAG-BNRF1 and HA-Daxx deletion constructs, visualized by Western blotting. The input (6%) of each IP is shown in the left. (C) IP assay of FLAG-tagged histone H3.1 or H3.3 with Daxx and BNRF1, analyzed by Western blotting. (B and C) Molecular masses (in kilodaltons) are shown on the left.

that Daxx interacts with H3.3 with greater affinity than with H3.1 (22). These results suggest that BNRF1, instead of disrupting Daxx-H3.3 binding, forms a complex with both Daxx and H3.3.

To further test the formation of a BNRF1/Daxx/H3.3 complex, the Daxx interaction domain (DID) of BNRF1 (40) was cloned as a GST-tagged construct (Fig. 2A). Purified bacterially produced GST-BNRF1-DID or GST alone was immobilized on glutathione-Sepharose beads and coincubated with nuclear protein extract from Mutu I human B cell-lymphoma cell lines. After extensive washing, interacting proteins were analyzed by Western blotting.

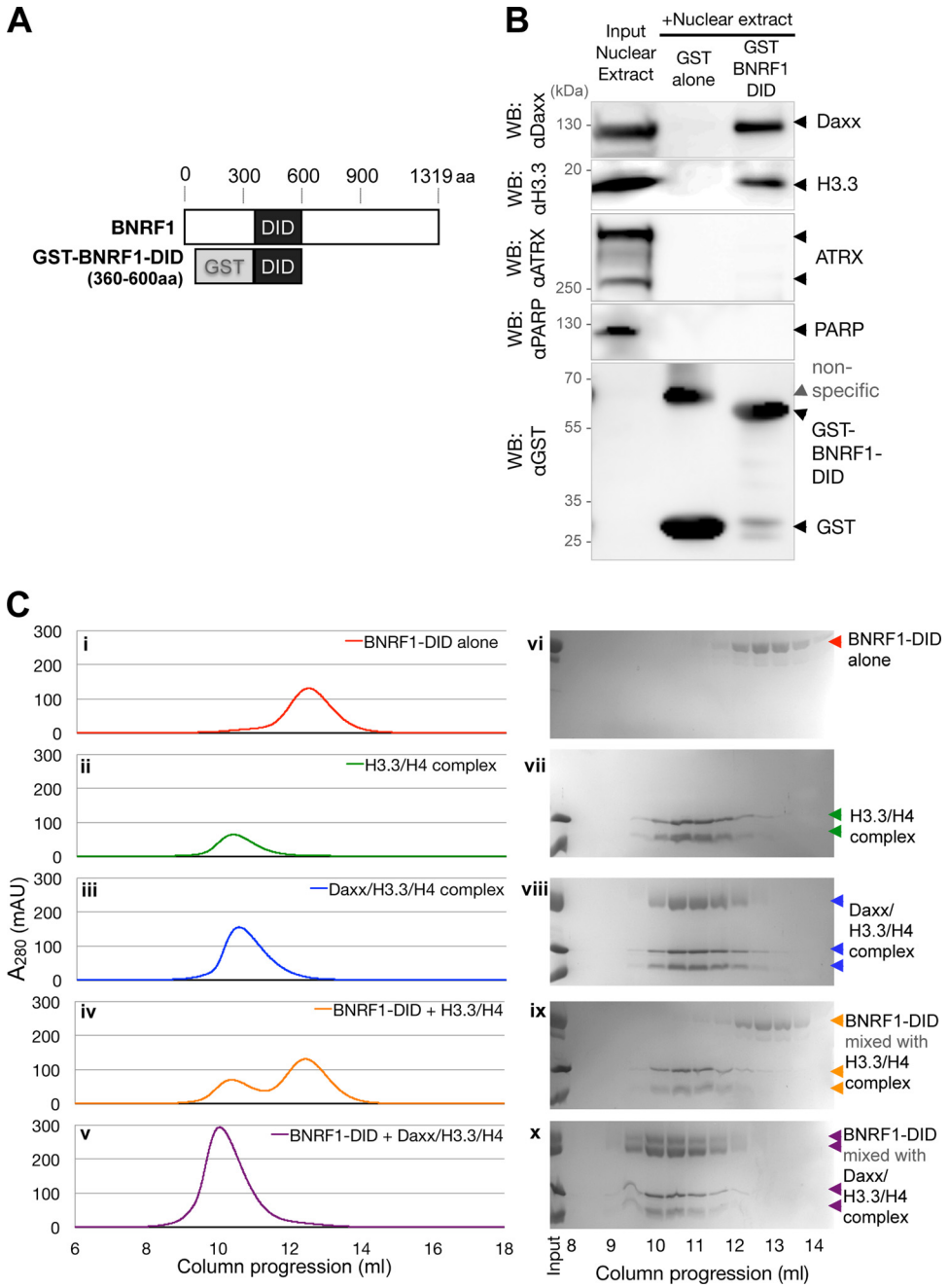

FIG 2 The Daxx interaction domain (DID) of BNRF1 forms a complex with the Daxx/H3.3/H4 complex. (A) Diagram of GST-tagged BNRF1 DID construct. (B) GST pulldown of BNRF1-interacting nuclear proteins. Purified GST-BNRF1-DID or GST alone was used to pulldown cellular proteins from Mutu I cell nuclear extract. Total nuclear extract (input) and eluted proteins from GST alone or GST-BNRF1-DID were analyzed by Western blotting and probed for Daxx, histone H3.3 and GST, with ATRX and PARP probed as negative controls. Molecular masses (in kilodaltons) are shown on the left. (C) (i to iv) Gel filtration chromatograms of BNRF1-DID and Daxx/H3.3/H4 complexes. Bacterially produced, purified BNRF1-DID, H3.3/H4 tetramer, and Daxx/H3.3/H4 complex were passed through a Superdex S75 column in different combinations. (vi to x) Fractions were collected and analyzed by SDS-PAGE and Coomassie blue staining.

Both Daxx and histone H3.3 bound to GST-BNRF1-DID but did not bind to the GST control (Fig. 2B). Complex formation was specific to Daxx and H3.3 since neither ATRX nor the nuclear enzyme poly(ADP-ribose) polymerase (PARP) were pulled down by GST-BNRF1-DID. These results further support the model that BNRF1 forms complexes with Daxx and histone H3.3.

To determine whether formation requires any additional cellular factors, purified BNRF1-DID was incubated with purified bacterially produced Daxx-HBD and recombinant histones H3.3 and H4. Complex formation was then analyzed by size-exclusion chromatography (Fig. 2C). As expected, H3.3/H4 ran with a stoichiometry of ~1:1, DAXX/H3.3/H4 as ~1:1:1, and BNRF1-DID as a monomer (~35 kDa). When BNRF1-DID was coincubated with preformed H3.3/H4 tetramers, the proteins migrated as dis-

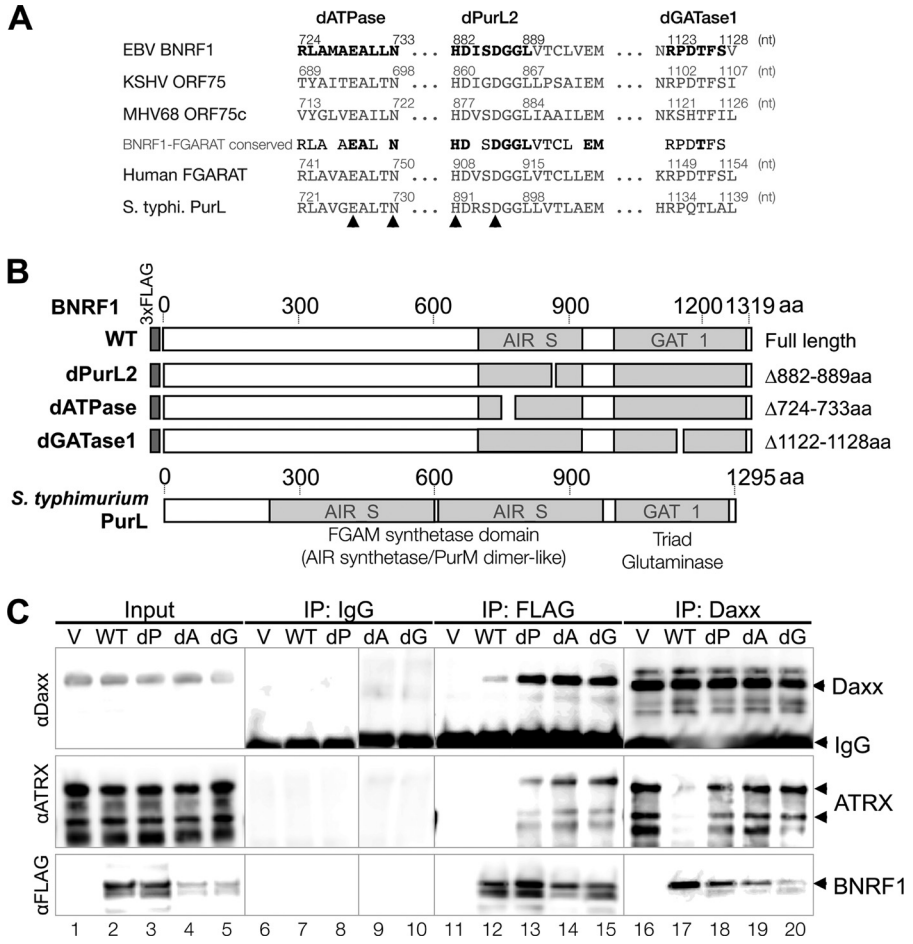

FIG 3 FGARAT homology domains of BNRF1 are essential for dissociation of ATRX from Daxx. (A) Sequence comparisons of EBV BNRF1 with other homologous genes, including KSHV ORF75, MHV68 ORF75c, human FGARAT, and *Salmonella* Typhimurium PurL. Arrowheads denote residues on *Salmonella* PurL that form hydrogen bonds with ADP (54). (B) Diagram of FLAG-BNRF1 constructs with deletions in FGARAT-homology conserved regions. (C) IP-Western assay of FLAG-tagged BNRF1 FGARAT-homology mutants in transfected 293T cells and probed for association with Daxx and ATRX.

tinctly separate peaks at positions identical to the individual components. However, when BNRF1-DID was incubated with preformed DAXX/H3.3/H4 complexes, the proteins comigrated, with an apparent stoichiometry close to 1:1 for BNRF1 with the DAXX/H3.3/H4 complex. This shift in mobility indicates that BNRF1 forms a cocomplex with Daxx and H3.3/H4. The findings also indicate that Daxx is required for BNRF1 interaction with histones H3.3 and H4.

The FGARAT homology domains of BNRF1 is important for Daxx-ATRX disruption. The selective conservation of FGARAT-like amino acid sequences at the C termini of all gammaherpesvirus BNRF1-ORF75 homologues suggests that this domain is functionally important for the gammaherpesvirus life cycle. Although we have not yet found a functional link of BNRF1 with the conserved function of FGARAT in purine metabolism, we tested if this enzyme homology is linked to the ability of BNRF1 to disrupt the Daxx-ATRX complex. To test this hypothesis, we introduced small deletions targeting regions of BNRF1 that are homologous to conserved functional domains in the FGARAT gene (Fig. 3A and B, aligned to the *Salmonella enterica* serovar Typhimurium homologue PurL). The dATPase (dA) and dPurL2 (dP) deletions target highly conserved domains with residues that were found to form hydrogen bonds with an ADP molecule cocrystalized with FGARAT (54), while the dGATase1 deletion (dG) covers residues important in the glutaminase domain of FGARAT. The ability of these mutants to interact with Daxx and disrupt Daxx-ATRX binding was tested by IP-Western blot assays performed on 293T cells transfected with empty FLAG vector (V), FLAG-tagged WT or enzymatic mutants (dP, dA, and dG) of BNRF1 (Fig. 3C). We found that WT and all enzymatic mutants of FLAG-BNRF1 coimmunoprecipitated with Daxx. However, in contrast to WT BNRF1, none of the mutants could disrupt ATRX interaction with Daxx (Fig. 3C, lane 17, ATRX panel). These results suggest that the FGARAT homology of BNRF1 is important for displacing ATRX from the Daxx-ATRX complex and thus critical for its biochemical function.

WT BNRF1, but not the d26 or dATPase mutants, mobilizes core histone H3.3. The observations that BNRF1 replaces ATRX from the Daxx-ATRX histone H3.3 loading complex suggest the possibility that BNRF1 may modulate the chromatin remodeling functions of Daxx, which should affect histone dynamics. Global histone dynamics can be measured in living cells using FRAP with fluorescently tagged histones (55). We sought to determine whether BNRF1 was sufficient to increase the pool of histone H3.3

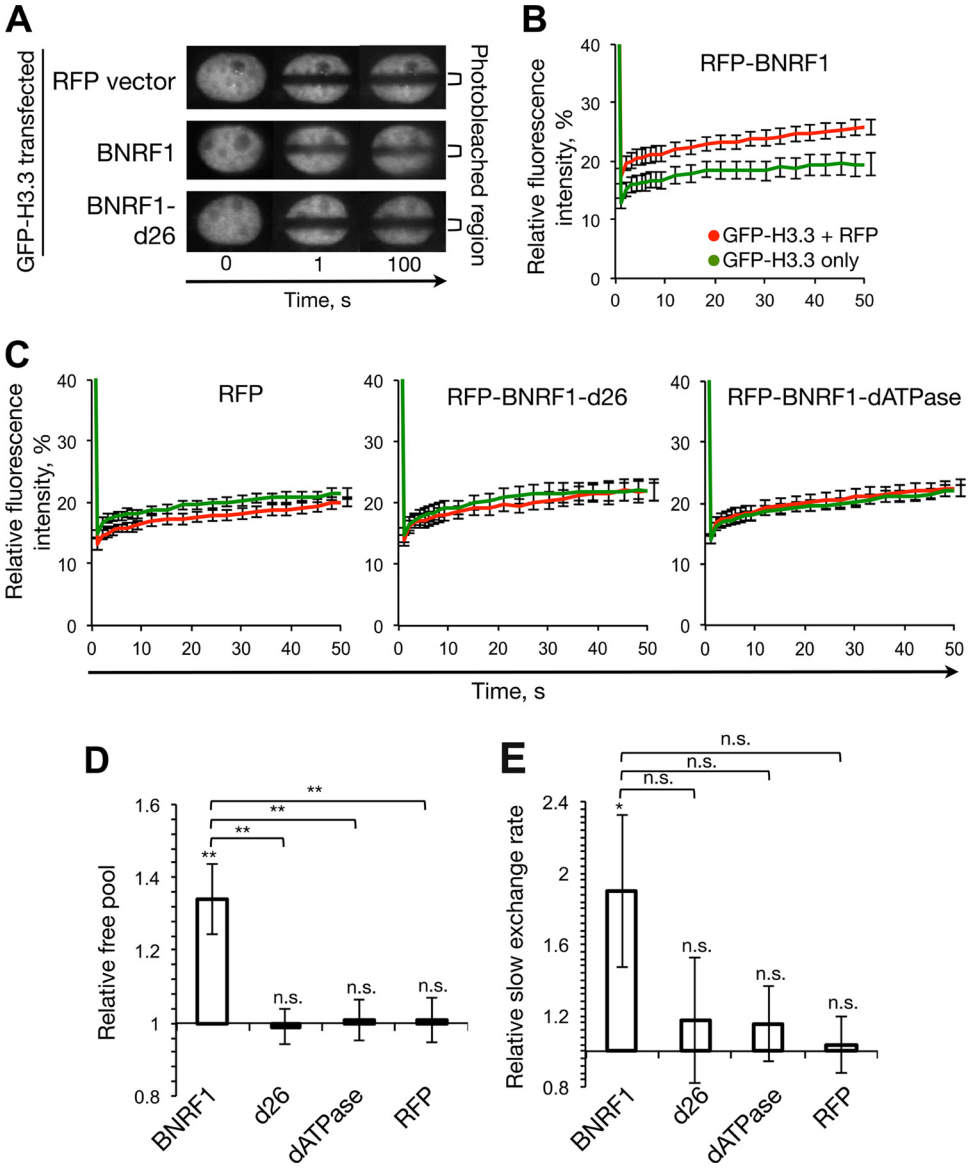

FIG 4 WT BNRF1 mobilizes histone H3.3, whereas the d26 or dATPase mutants do not. (A) Images of nuclei expressing GFP-H3.3 only, or GFP-H3.3 and WT or d26 BNRF1, at three different time points. Time (T) = 0 s is immediately prior to photobleaching, T = 1 s is immediately after photobleaching. The relative fluorescence of the photobleached region at T = 1 s is representative of the free pool of GFP-H3.3. (B and C) FRAP analysis of histone H3.3 in cells expressing detectable levels of RFP-BNRF1 compared to cells with no detectable RFP signal. Line graphs present the relative normalized fluorescence intensity of the photobleached nuclear region plotted against time; averages ± the standard errors of the mean (SEM) are indicated. Signal readouts from cells that coexpressed detectable levels of GFP-H3.3 and WT (B) or d26, dATPase RFP-BNRF1, or free RFP (C) are shown in red; signal readouts from cells that expressed detectable levels of only GFP-H3.3 are shown in green. (D) Bar graphs present the free pool of GFP-H3.3 in cells expressing detectable levels of WT, d26, or dATPase RFP-BNRF1 or free RFP, relative to the levels in cells expressing detectable levels of only GFP-H3.3 on the same coverslip; averages ± the SEM are shown. *, $P < 0.05$; **, $P < 0.01$. (E) Average slow GFP-H3.3 exchange rate in cells expressing detectable levels of WT, d26, or dATPase RFP-BNRF1, or free RFP, relative to cells expressing detectable levels of only GFP-H3.3 on the same coverslip; averages ± the SEM are shown. *, $P < 0.05$; **, $P < 0.01$.

not bound in chromatin at any given time and whether this mechanism was dependent on the Daxx interaction or the putative ATPase domain. We evaluated the kinetics of FRAP of GFP-H3.3 (44), which is loaded onto chromatin by the Daxx-ATRX complex (22). Cells expressing detectable levels of WT BNRF1 had significantly faster fluorescence recovery in the photobleached region than cells not expressing detectable levels of WT RFP-BNRF1 (Fig. 4A and B, compare red to green lines). In contrast, this accelerated fluorescence recovery was not observed in cells expressing detectable levels of RFP-BNRF1-d26, RFP-BNRF1-dATPase, or free RFP (Fig. 4C).

Mobilization of GFP-H3.3 in cells that coexpressed detectable levels of WT or mutant RFP-BNRF1 was next normalized to their mobilization in BNRF1-nonexpressing cells on the same coverslip. We then analyzed the relative fluorescence intensity of the photobleached nuclear region immediately after photobleaching, which reflects the pool of free histones. We found that BNRF1 was sufficient to increase the free pool of H3.3 by 34% ± 10% ($P <$

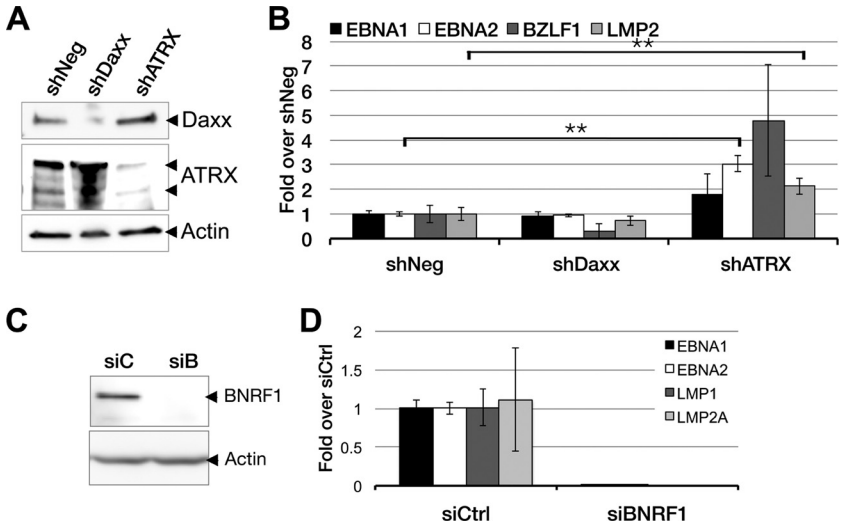

FIG 5 Viral gene expression in the prelatency phase is repressed by ATRX in the absence of BNRF1. (A) Western blot validation of shRNA-mediated Daxx or ATRX depletion in EBV-negative Akata cells, with nontargeting shNeg as a negative control. (B) qPCR assay of viral gene expression in Daxx/ATRX-depleted EBV-infected cells. EBV-negative Akata cells with Daxx or ATRX depleted were infected with ΔBNRF1-bacmid produced virus and collected 48 hpi for qRT-PCR quantification of mRNA levels. **, Statistical significance ($P < 0.01$) as determined by a one-tailed Student *t* test. Error bars indicate the standard deviations (SD). (C) Confirmation of siRNA-mediated BNRF1 depletion in virus producer 293 cells by Western blotting. Wild-type or BNRF1-knocked-down virus was collected from 293 producer cells stably transfected with EBV genomes and treated with control (siCtrl) or BNRF1-specific siRNA (siBNRF1). This batch of virus was used for the ChIP assays in Fig. 8A. (D) qPCR assay of latent viral gene expression in siCtrl or siBNRF1 EBV-infected primary B lymphocytes collected at 72 hpi.

0.01) (Fig. 4D). In contrast, the free pool of H3.3 showed no significant changes in d26, dATPase, or RFP vector-expressing cells.

The slow exchange rate of H3.3 was also studied by analyzing the fluorescence recovery rate at the later times, 20 to 100 s after photobleaching. H3.3 slow exchange rate was 90% ± 43% greater in cells expressing detectable levels of WT BNRF1 than in those with no detectable BNRF1 ($P < 0.05$). In contrast, the rate was not greater in cells expressing detectable levels of d26, dATPase, or free RFP than in cells expressing detectable levels of only GFP-H3.3 (Fig. 4E). However, the variability in the slow exchange rates did not allow reaching statistical significance when we compared WT to mutant forms of BNRF1.

Thus, WT BNRF1 is sufficient to mobilize histone H3.3, increasing their levels available in the free pools and augmenting H3.3 slow chromatin exchange rates. The Daxx-interaction-deficient (d26) or ATRX-disruption-deficient (dATPase) mutants, in contrast, are unable to induce H3.3 mobilization.

Higher levels of viral gene expression during early infection in the absence of ATRX. ATRX and Daxx has been associated with antiviral resistance in the form of repression of HSV-1 and HCMV viral gene expression (56, 57), while Daxx-ATRX loaded histone H3.3 has also been linked with gene repression of a CMV promoter-driven plasmid (58). We reasoned that the disruption targets of BNRF1, Daxx and ATRX, may repress EBV gene expression. To test this, we measured viral gene expression during EBV primary infection of cells with Daxx or ATRX knocked down. For these shRNA depletion experiments, we utilized an EBV-negative Akata Burkitt lymphoma cell line that could be selected after lentivirus shRNA infection and subsequently infected with EBV to evaluate early events after primary infection. EBV-negative Akata B cells were transduced with shRNA-expressing lentivirus, targeting Daxx (shDaxx), ATRX (shATRX), and also a nontargeting shRNA (shNeg). Knockdown efficiencies are shown in Fig. 5A. shRNA-expressing cells were then infected with EBV virus produced from BNRF1-null (ΔBNRF1) bacmids (39). Infected cells were harvested 72 hpi, and viral mRNA levels were analyzed by RT-qPCR (Fig. 5B). When ATRX was knocked down (shATRX), there was a significant increase in viral latent gene expression levels (specifically EBNA2 and LMP2). However, the effects of shATRX on BZLF1 expression were too small to reach statistical significance. Whereas the knockdown of Daxx (shDaxx) did not show any significant difference from the negative control (shNeg). These results suggest that ATRX is a repressor of EBV prelatency gene expression during primary infection and that BNRF1 is required to neutralize ATRX-mediated repression.

BNRF1 siRNA-depleted virus fails to produce latent transcripts. With BNRF1 forming an alternate complex with Daxx-histones and mobilizing histones, we aimed to study the effects of BNRF1 on viral chromatin assembly in the early establishment of EBV latent infection. Previous studies utilized a recombinant EBV with a truncation in the BNRF1 gene, which was characterized to be unable to express viral genes upon primary infection of B lymphocytes (39). To overcome technical difficulties we encountered with producing virus from the BNRF1-truncated bacmid, we generated BNRF1 depleted virus by using siRNA during viral production from the WT EBV bacmid. 293 cells stably carrying the EBV genome bacmid were transfected with the EBV transactivator Zta and BALF4 to induce viral production. These virus production cells were also cotransfected with nontargeting (siCtrl) or BNRF1-targeting (siBNRF1) siRNA. The knockdown efficiency in virus producer cells is shown in Fig. 5C. Since only the protein, but not the coding DNA, of BNRF1 is repressed by siRNA, any phenotype of siBNRF1 is likely due to the lack of tegument-delivered, rather than *de novo*-synthesized BNRF1 or any potential defect on the viral genome. This method also improved the production and infectivity of BNRF1-null virus. We first tested the siBNRF1 virus infection system to evaluate whether the absence of BNRF1 protein in the tegument also resulted in gene expression failure. Viruses that infected B

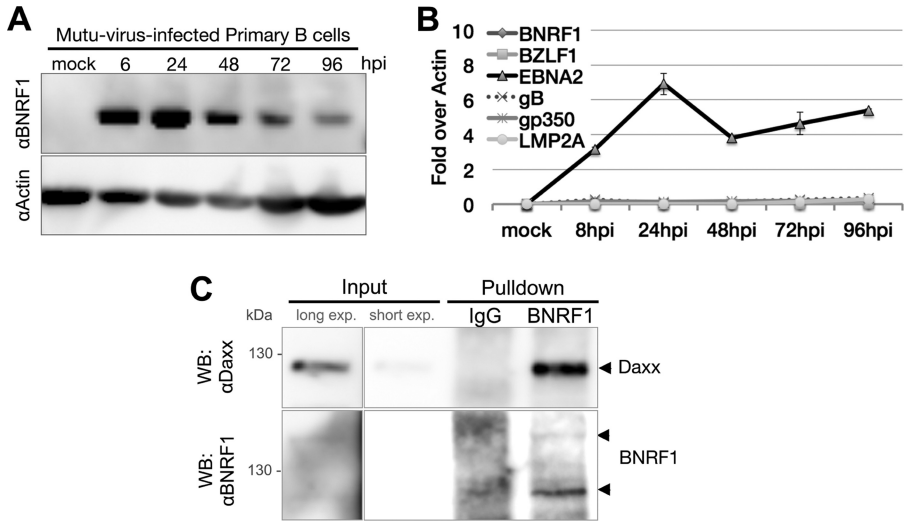

FIG 6 Tegument-derived BNRF1 is stable and interacts with Daxx during early infection, whereas no *de novo* expression of BNRF1 could be detected. Mutu I strain EBV-infected primary B lymphocytes in the prelatency phase were collected in a time course and subject to Western blot analysis of BNRF1 protein (A) and qPCR assay of viral gene transcripts (B). Error bars indicate the SD. (C) EBV-infected B cells were collected 2 days postinfection and subject to immunoprecipitation with BNRF1 antibody-conjugated beads.

cells in the absence of BNRF1 (siBNRF1) failed to express several latency-associated viral genes, including EBNA2, EBNA1, LMP1, and LMP2A (Fig. 5D), as expected (40). These results indicate that the absence of BNRF1 protein in the tegument results in a failure of viral gene expression during early infection.

Native BNRF1 protein interacts with Daxx during early infection of primary B lymphocytes. To better understand the function of BNRF1 during primary infection, we first assayed the expression levels of BNRF1 during *de novo* infection. Primary B cells were infected with Mutu I derived virus and infected cells extracts were assayed by Western blotting at various times. We found that BNRF1 protein levels peak at ~24 hpi and then diminish to a much lower, but clearly detectable levels by 96 hpi (Fig. 6A). This suggests that BNRF1 may be supporting infection up to 2 to 4 days postinfection. The slight increase in BNRF1 at 24 hpi relative to 6 hpi may result from additional cell infections during this time, or it could be due to *de novo*-produced BNRF1. To test the latter possibility, we tested Mutu-infected B cells for the presence of viral mRNA transcripts (Fig. 6B). As controls, we tested the immediate-early gene BZLF1, the latent genes EBNA2 and LMP2A, and late genes gB and gp350. In accordance with prior reports (59), EBNA2 mRNA could be detected as early as 8 hpi, whereas all other genes, including BNRF1, were not detectable up to 96 hpi. To understand the protein interactions of native BNRF1, we harvested more EBV-infected primary B cells at 2 days postinfection and assayed BNRF1-Daxx interaction by immunoprecipitation with anti-BNRF1 antibody-conjugated beads (Fig. 6C). We found that Daxx could indeed be pulled down with BNRF1 antibodies, but not by control IgG, from these extracts. We conclude that during early infection in B cells, the majority of BNRF1 is tegument derived, that this BNRF1 is stable enough to persist through the first 3 days postinfection, and that native virus-delivered BNRF1 could interact with cellular Daxx.

Tegument-delivered BNRF1 disperses Daxx/ATRX and prevents Daxx/ATRX from localizing next to viral DNA upon primary infection. Biochemical protein interaction assays suggest that BNRF1 disassembles Daxx-ATRX. However, we have not shown direct evidence of BNRF1 disruption of Daxx-ATRX in primary infection. It was also unclear whether the siBNRF1 virus could deliver its genome into the host nucleus. We thus tested infection of primary B lymphocytes using virus produced in siBNRF1 or siCtrl-treated cells and stained the infected cells for Daxx or ATRX and EBV viral DNA by immunofluorescence coupled with fluorescent *in situ* hybridization (IF-FISH) at the 72-hpi time point. Infected cells were stained with Daxx or ATRX antibodies (red signal) and then the viral genomes were *in situ* hybridized with prelabeled EBV viral DNA fragments (green signal). FISH signals were present in infected cell nuclei regardless of the presence or absence of BNRF1, indicating that genomes are delivered to the nucleus in the absence of BNRF1 (Fig. 7A and B). Furthermore, we found two phenotypes of ATRX and Daxx nuclear staining patterns (Fig. 7): highly speckled nuclear bodies and less distinct foci with a highly dispersed background staining. Both speckled and dispersed patterns were expected regardless of infection conditions, since nuclear bodies were known to be disassembled during mitosis (60). However, the dispersed patterns looked reminiscent of the dispersed ATRX foci in 293T cells transiently transfected with FLAG-BNRF1 (40) and was likely to be increased as a result of BNRF1-mediated disruption (Fig. 7Aii and Bii). Indeed, there was a significantly higher rate (71%) of dispersed ATRX pattern (Fig. 7A) in infections in the presence of BNRF1 (siCtrl) than in the absence of BNRF1 (siBNRF1). When the speckled versus dispersed patterns in infected cells (green FISH signal positive) were quantified (Fig. 7C), we found a significantly higher rate (71%) of dispersed ATRX pattern (Fig. 7A) in infections in the presence of BNRF1 (siCtrl) than in the absence of BNRF1 (siBNRF1, 38%) (Fig. 7C). The rate of Daxx dispersion (Fig. 7B and C) was also higher in siCtrl (73%)- than in siBNRF1 (26%)-infected cells, as expected. These results suggest that tegument-delivered BNRF1 displaces both Daxx and ATRX during primary infection, likely preventing their transcriptional repression and antiviral resistance activities. In the absence of BNRF1 (siB-

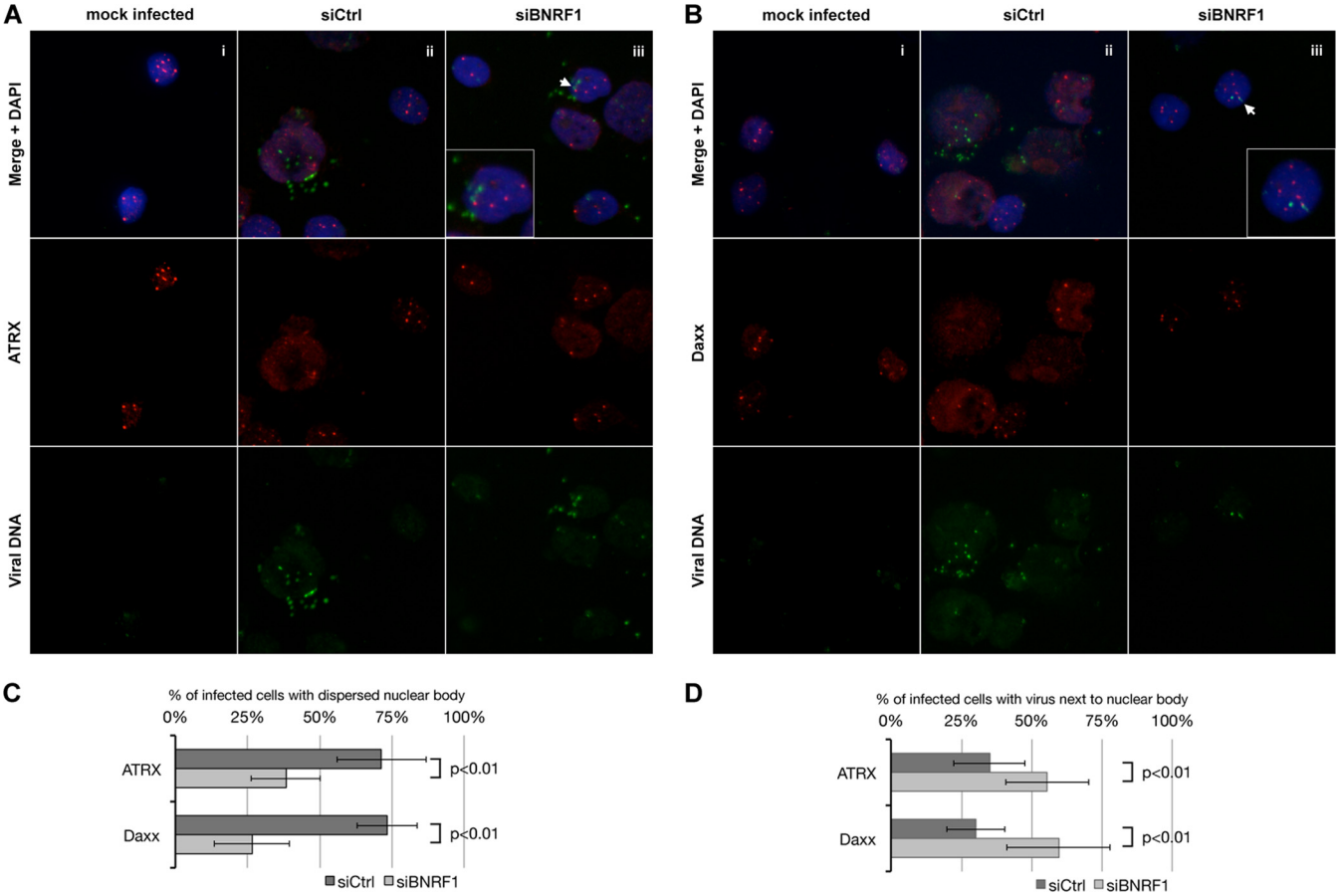

FIG 7 BNRF1-depleted virus infection showed less Daxx/ATRX dispersion and more viral DNA located next to Daxx/ATRX foci. siCtrl, siBNRF1 EBV-infected or mock-infected primary B lymphocytes in the pre-latent phase (72hpi) were subject to IF-FISH to visualize the infecting viral DNA in green, in conjunction with ATRX (A) or Daxx (B) in red. Cell nuclei were visualized with the blue DNA stain, DAPI. In siBNRF1 infections, arrowheads indicates where viral DNA is localizing adjacent to ATRX (Aiii) or Daxx (Biii) foci, insets showing zoomed-in views of the adjacent event. (C) Bar graph showing percentage of infected cells (green positive) with dispersed (high nuclear background red signals with weak foci) ATRX or Daxx signals. (D) Percentage of infected cells with ATRX or Daxx adjacent to viral DNA (red foci next to green foci). Approximately 60 to 100 infected cells counted per slide. Statistical significance was determined by using a one-tailed Student *t* test; error bars indicate the SD.

NRF1), we also noticed an increase of viral DNA localizing right next to Daxx or ATRX foci (Fig. 7Aiii, Biii, and D), supporting the ChIP findings that BNRF1 prevents Daxx and ATRX association with viral chromatin. These data suggest that through spatial relocalization of Daxx and ATRX, tegument-delivered BNRF1 could disrupt Daxx-ATRX-mediated resistances *in vivo* during primary infection.

BNRF1 prevents ATRX and H3.3 loading while promoting active chromatin marks on viral chromatin. EBV viral DNA enters the cell devoid of histones, and H3.3 is the only histone H3 variant that is loaded independently of DNA replication (25). Since Daxx selectively loads histone variant H3.3, we hypothesize that BNRF1-dependent disruption of Daxx-ATRX may prevent or regulate histone H3.3 loading on viral chromatin. We tested this model using ChIP assays on B lymphocytes infected with EBV in the presence (siCtrl) or absence of BNRF1 (siBNRF1). Infected human primary B cells were collected at 72 hpi and cross-linked. At 72 hpi, tegument-delivered BNRF1 is just starting to decay, while the first expressed latent gene EBNA2 has started to be expressed. Several EBV loci were tested, including a CTCF binding site next to the terminal repeats (CTCF 166), the first activated latent promoter Wp, the immediate-early promoter Zp, and a region in the EBNA2 gene body as an example of a region that is presumably less regulated. H3.3 chromatin binding increased in cells infected with BNRF1-knockdown (siBNRF1) virus compared to WT (siCtrl) virus (Fig. 8A, top two panels). We tested whether the change in H3.3 loading was associated with changes in histone chaperone access to viral genome. ATRX and Daxx binding on viral DNA was increased in the absence of BNRF1 (siBNRF1) (Fig. 8B). H3.3, Daxx, and ATRX binding was elevated at most viral loci tested in the siBNRF1 virus-infected cells. Of all sites tested, the most prominent enrichment of H3.3 was located at Wp, which is among the earliest activated viral promoters driving EBNA2 expression in the prelatency phase (61).

H3.3 loading increased and viral gene expression was inhibited in siBNRF1 infected cells. However, H3.3 association with active or repressive chromatin appears to be genomic region and chaperone dependent. We thus further tested by ChIP, the presence of active (H3K4me3) and repressive (H3K9me3) chromatin markers on viral genomes during early infection (Fig. 8A, lower two panels). Although no H3K9me3 was found on early infection viral genomes, we found more H3K4me3 active markers in cells infected in the presence of BNRF1 (siCtrl) then in the absence of

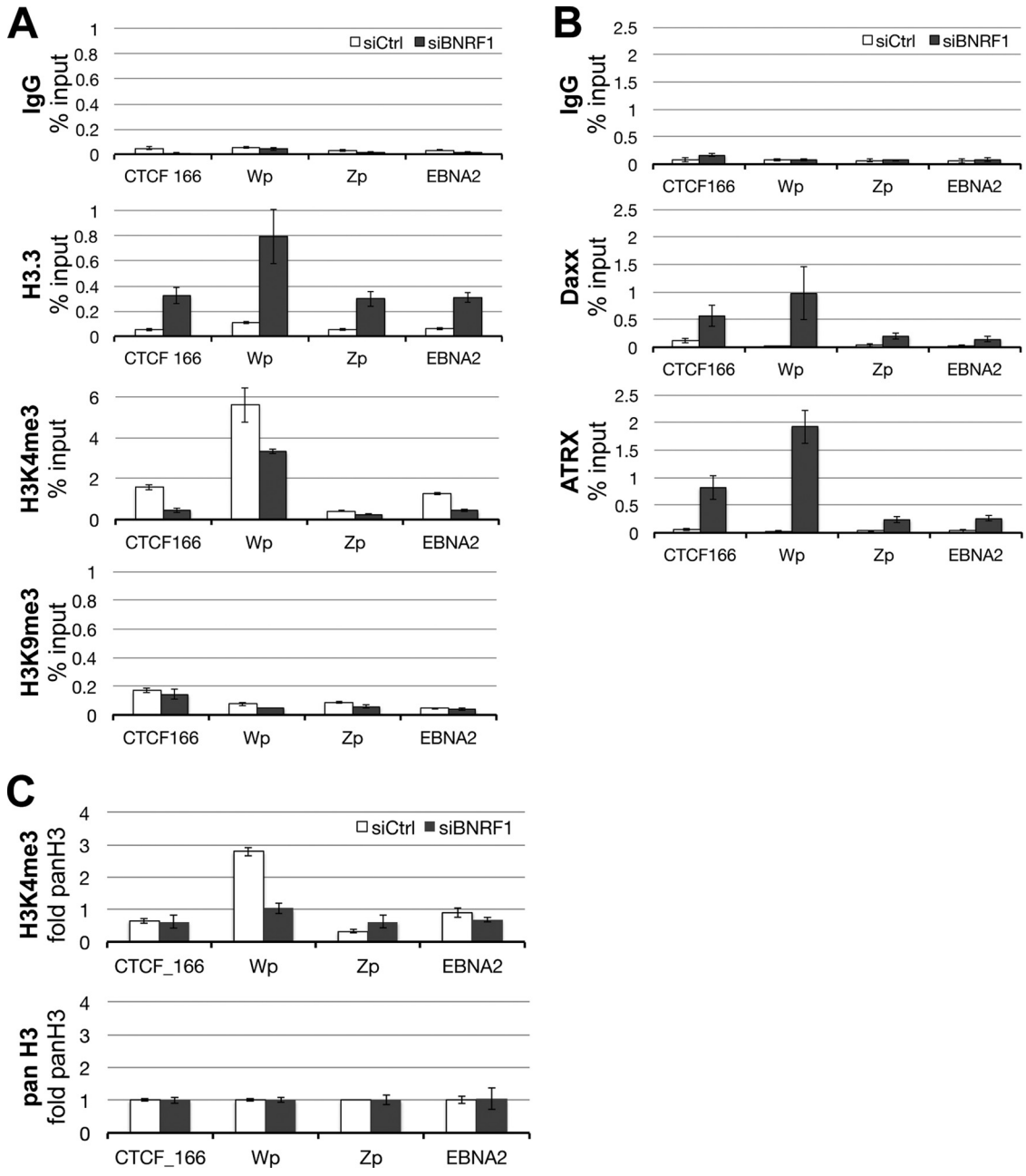

FIG 8 BNRF1 decreases histone H3.3, Daxx, and ATRX binding and promotes H3K4me3 accumulation in viral genomic regions. BNRF1-depleted EBV-infected primary B lymphocytes in the prelatency phase were tested for histone H3.3, Daxx, and ATRX binding on viral DNA. Human primary B lymphocytes infected with siCtrl- or siBNRF1-treated cell-produced virus were collected at 72 hpi and subjected to ChIP to test for H3.3, H3K4me3, and H3K9me3 (A) and Daxx or ATRX (B) binding on viral genomic regions by qPCR. The regions tested included the following: a CTCF binding site close to the terminal repeats (CTCF 166); the W promoter (Wp), which drives EBNA2 expression in the prelatency phase; the Z promoter (Zp), which drives the immediate-early gene Zta; and a region in the EBNA2 gene body. Error bars indicate the SD. (C) Bar graph of ChIP signals of H3K4me3 or pan-H3 on siCtrl or siBNRF1 virus-infected primary B cells, normalized to the average pan-H3 values.

BNRF1 (siBNRF1). To control for different levels of histone H3 on viral genomes in the two infection sets, we tested H3K4me3 and pan-histone H3 binding, alternatively analyzing the H3K4me3 ChIP levels normalized to total histone H3 levels in the same region (Fig. 8C). The increased presence of H3K4me3 on viral control regions in cells infected with BNRF1-knockdown (siBNRF1) virus compared to wild-type (siCtrl) virus was also evident in the normalized data. These results suggests that BNRF1, which dissociates ATRX from Daxx, inhibits the deposition of histone H3.3, increases the active marker H3K4me3 on the viral genome, and in turn promotes the viral gene expression required for latency establishment during early infection.

DISCUSSION

DNA viruses may require host chromatin regulatory processes to protect and regulate their genomes, and yet these same host pro-

cesses can form repressive chromatin that blocks viral gene expression. In this respect, chromatin remodeling processes become a critical point of conflict between host and virus. Herpesvirus-encoded tegument proteins play a key role in regulating viral gene expression during early infection, typically targeting host intrinsic resistances such as PML-NBs. Here, we find that the EBV-encoded tegument protein BNRF1 modulates viral chromatin assembly by altering the histone H3.3 chaperone complex of Daxx-ATRX. We find that BNRF1 replaces the histone cochaperone ATRX to form a ternary complex of BNRF1, Daxx, and histone H3.3/H4 but not histone H3.1. Mutations in motifs conserved across gammaherpesviruses prevent BNRF1 from displacing ATRX from Daxx while retaining the Daxx-interaction function. BNRF1 can mobilize and increase the free pool of histone H3.3, an activity that is lost in ATRX disruption-deficient mutants. IF-FISH and ChIP assays on primary infection reveal that BNRF1 prevents Daxx/ATRX-mediated assembly of histone H3.3 and promotes more active histone marks at key regulatory elements in the viral genome. Taken together, these findings support a model whereby EBV tegument protein BNRF1 modulates a host histone chaperone complex to ensure the expression of essential viral latent genes. These findings suggest that ATRX-associated chromatin assembly acts as an intrinsic antiviral resistance that can be disabled by tegument proteins like BNRF1to promote viral gene expression programs.

The chromatin-associated factors that BNRF1 targets have important functions in cellular gene regulation and genome maintenance. Mutations in Daxx, ATRX, and H3.3 are found with high frequency in several human cancers (62, 63). Mutations in these factors have been correlated with an increase in homologous recombination and the alternative lengthening of telomere (ALT) in these cancer cells (64). The histone variant H3.3 is assembled in a DNA replication-independent manner by the histone chaperones HIRA or Daxx-ATRX. Loading of H3.3 by HIRA is associated with transcription activity (25). On the other hand, loading of histone H3.3 by Daxx-ATRX is associated transcriptional repression, particularly at repetitive GC-rich telomeric repeats (26), pericentric DNA repeats (65), and a CMV promoter-driven transgene array (58). Mutations in ATRX are also known to cause alpha-globin thalassemias and X-linked mental retardation syndromes where the underlying pathogenesis has been linked to defective chromatin assembly at repetitive DNA (66).

Daxx, ATRX, and H3.3 have also been implicated in the control of viral gene expression during infection. Herpesviral DNA in virions is devoid of histones (67) and is only loaded with histones after entry in the nucleus. For HSV-1, histone H3.3 is loaded on the viral genome immediately upon nuclear entry and then replaced with histone H3.1 after initiation of viral DNA synthesis (68). For human CMV, Daxx silencing prior to infection resulted in a decrease of heterochromatic marks on the major viral immediate-early promoter (MIEP) and an increase in viral gene expression (28). Similarly, Ad5 encodes proteins that target ATRX degradation to prevent the assembly of H3.3 and transcriptional repression of essential viral genes (29). Taken together, these reports suggest that Daxx-ATRX loading of H3.3 contributes to antiviral resistance by establishing repressive heterochromatin on viral genomes.

The findings presented here indicate that BNRF1 prevents repressive chromatin formation onto the EBV genome during primary infection of B lymphocytes. Both ChIP and IF-FISH assays demonstrate that Daxx, ATRX, and histone H3.3 occupancy at the viral genome increases after infection with virus prepared from BNRF1-depleted cells (Fig. 6 and 7). The BNRF1-dependent decrease in H3.3 loading on the viral genome is consistent with the FRAP observation that BNRF1 increases the free pool of H3.3 (Fig. 4B). We also show that BNRF1-deficient virus can be partially rescued in host cells with ATRX depleted (Fig. 5B). Surprisingly, depletion of Daxx did not result in the rescue of BNRF1-deficient virus, suggesting that ATRX is the limiting factor or that Daxx and ATRX have nonredundant functions in viral gene regulation. Regardless, our findings suggest that ATRX is a principal restriction factor for EBV chromatin regulation during primary infection. We propose that BNRF1 selectively replaces ATRX from the Daxx-H3.3/H4 complex to prevent the assembly of repressive H3.3 chromatin on the viral genome.

The importance of BNRF1 to viral infection and gene expression is underscored by its evolutionarily conservation among all gammaherpesvirus family members. All known gammaherpesviruses contain a BNRF1 homologue found in the tegument, including KSHV ORF75, HVS ORF3, and MHV68 ORF75c (Fig. 3A). The homology is found exclusively in a domain that contains sequence homology to a cellular purine biosynthesis enzyme, FGAR-AT, which hydrolyzes ATP to transfer an amino (NH_2) group from glutamine to its substrate. The precise function of this FGAR-AT domain in viral proteins is not yet known. Nevertheless, we found that the conserved ATPase and glutamine amidotransferase (GATase1) domains were important for disrupting ATRX from the Daxx-histone complex (Fig. 3C). All viral FGARAT family members target PML-NBs. However, each of these proteins functions through different mechanisms of disrupting PML-NB function. The MHV68 ORF75c degrades PML (37), and HVS ORF3 degrades Sp100 (38). Although KSHV ORF75 does not interact directly with Daxx, it has recently been found to relocate PML and Sp100 away from PML-NBs and likely degrades ATRX during both early infection and lytic reactivation in an endothelial cell line (36). Notably, all reports of viral FGARAT-induced protein degradations were investigated in epithelial model systems where gammaherpesviruses preferentially undergo lytic replication shortly after infection. In our study, we focused on the effects of EBV BNRF1 in B lymphocytes, where a programmed latency is the predominant outcome. BNRF1 showed a nondegradation pathway of modifying Daxx-ATRX in these cells. Cell type dependencies were similarly observed for HCMV tegument protein pp71, which disrupted Daxx-mediated repression in differentiated cells supporting productive infection and yet failed to prevent repression in undifferentiated cells where productive infection was not supported (69, 70). Therefore, a comparison of BNRF1 function in lymphocytes versus epithelial cell types may shed light onto the mechanism whereby EBV enters latency or lytic replication cycles.

In conclusion, we show that the host antiviral resistance orchestrated by Daxx, ATRX, and histone H3.3 can be altered by EBV tegument protein BNRF1. BNRF1 replaces ATRX in the Daxx-ATRX histone chaperone complex and can stimulate the global mobilization of histone H3.3. BNRF1 is essential for the early steps of viral infection since its absence results in increased Daxx, ATRX, and H3.3 binding on viral chromatin and shutdown of latent viral gene expression. BNRF1 controls the process of viral chromatin assembly in preparation for the establishment of persistent latent infection by EBV. These findings also demonstrate that host chromatin assembly is an important form of host cell intrinsic resistance to viral infection.

ACKNOWLEDGMENTS

We thank the Wistar Institute Cancer Center Core Facilities for Microscopy, Genomics, and Molecular Screening for help with imaging and analysis, DNA sequencing, and lentiviral vector production. We especially thank Frederick S. Keeney from the Wistar Microscopy Core Facility for help and discussions on microscopy and image analysis. We acknowledge the contributions of Hsiu-Ming Shih, Dinshaw Patel, and Roger Everett. We also thank Hongda Huang of the Patel lab for discussions on the FGARAT homology of BNRF1 and Italo Tempera for discussions on assaying viral chromatin assembly.

This work was funded by grants from the National Institutes of Health (DE 017336, CA 093606, and P01 CA174439) to P.M.L. and AG031862 to R.M. and from CIHR (MOP106452) to L.M.S. L.M.S. is a Burroughs-Wellcome Fund Investigator in the Pathogenesis of Infectious Disease.

REFERENCES

1. **Burgess RJ, Zhang Z.** 2013. Histone chaperones in nucleosome assembly and human disease. Nat. Struct. Mol. Biol. **20:**14–22. http://dx.doi.org/10.1038/nsmb.2461.
2. **Knipe DM, Lieberman PM, Jung JU, McBride AA, Morris KV, Ott M, Margolis D, Nieto A, Nevels M, Parks RJ, Kristie TM.** 2013. Snapshots: chromatin control of viral infection. Virology **435:**141–156. http://dx.doi.org/10.1016/j.virol.2012.09.023.
3. **Knipe DM, Cliffe A.** 2008. Chromatin control of herpes simplex virus lytic and latent infection. Nat. Rev. Microbiol. **6:**211–221. http://dx.doi.org/10.1038/nrmicro1794.
4. **Saffert RT, Kalejta RF.** 2008. Promyelocytic leukemia-nuclear body proteins: herpesvirus enemies, accomplices, or both? Future Virol. **3:**265–277. http://dx.doi.org/10.2217/17460794.3.3.265.
5. **Boutell C, Everett RD.** 2013. Regulation of alphaherpesvirus infections by the ICP0 family of proteins. J. Gen. Virol. **94:**465–481. http://dx.doi.org/10.1099/vir.0.048900-0.
6. **Everett RD, Chelbi-Alix MK.** 2007. PML and PML nuclear bodies: implications in antiviral defence. Biochimie **89:**819–830. http://dx.doi.org/10.1016/j.biochi.2007.01.004.
7. **Bernardi R, Pandolfi PP.** 2007. Structure, dynamics and functions of promyelocytic leukaemia nuclear bodies. Nat. Rev. Mol. Cell. Biol. **8:**1006–1016. http://dx.doi.org/10.1038/nrm2277.
8. **Maul GG, Negorev D, Bell P, Ishov AM.** 2000. Review: properties and assembly mechanisms of ND10, PML bodies, or PODs. J. Struct. Biol. **129:**278–287. http://dx.doi.org/10.1006/jsbi.2000.4239.
9. **Wilcox KW, Sheriff S, Isaac A, Taylor JL.** 2005. SP100B is a repressor of gene expression. J. Cell. Biochem. **95:**352–365. http://dx.doi.org/10.1002/jcb.20434.
10. **Newhart A, Negorev DG, Rafalska-Metcalf IU, Yang T, Maul GG, Janicki SM.** 2013. Sp100A promotes chromatin decondensation at a cytomegalovirus-promoter-regulated transcription site. Mol. Biol. Cell **24:**1454–1468. http://dx.doi.org/10.1091/mbc.E12-09-0669.
11. **Lehembre F, Muller S, Pandolfi PP, Dejean A.** 2001. Regulation of Pax3 transcriptional activity by SUMO-1-modified PML. Oncogene **20:**1–9. http://dx.doi.org/10.1038/sj.onc.1204063.
12. **Emelyanov AV, Kovac CR, Sepulveda MA, Birshtein BK.** 2002. The interaction of Pax5 (BSAP) with Daxx can result in transcriptional activation in B cells. J. Biol. Chem. **277:**11156–11164. http://dx.doi.org/10.1074/jbc.M111763200.
13. **Li R, Pei H, Watson DK, Papas TS.** 2000. EAP1/Daxx interacts with ETS1 and represses transcriptional activation of ETS1 target genes. Oncogene **19:**745–753. http://dx.doi.org/10.1038/sj.onc.1203385.
14. **Michaelson JS, Leder P.** 2003. RNAi reveals antiapoptotic and transcriptionally repressive activities of DAXX. J. Cell Sci. **116:**345–352. http://dx.doi.org/10.1242/jcs.00234.
15. **Michaelson JS, Bader D, Kuo F, Kozak C, Leder P.** 1999. Loss of Daxx, a promiscuously interacting protein, results in extensive apoptosis in early mouse development. Genes Dev. **13:**1918–1923. http://dx.doi.org/10.1101/gad.13.15.1918.
16. **Li H, Leo C, Zhu J, Wu X, O'Neil J, Park EJ, Chen JD.** 2000. Sequestration and inhibition of Daxx-mediated transcriptional repression by PML. Mol. Cell. Biol. **20:**1784–1796. http://dx.doi.org/10.1128/MCB.20.5.1784-1796.2000.
17. **Hollenbach AD, McPherson CJ, Mientjes EJ, Iyengar R, Grosveld G.** 2002. Daxx and histone deacetylase II associate with chromatin through an interaction with core histones and the chromatin-associated protein Dek. J. Cell Sci. **115:**3319–3330.
18. **Muromoto R, Sugiyama K, Takachi A, Imoto S, Sato N, Yamamoto T, Oritani K, Shimoda K, Matsuda T.** 2004. Physical and functional interactions between Daxx and DNA methyltransferase 1-associated protein, DMAP1. J. Immunol. **172:**2985–2993. http://dx.doi.org/10.4049/jimmunol.172.5.2985.
19. **Picketts DJ, Higgs DR, Bachoo S, Blake DJ, Quarrell OW, Gibbons RJ.** 1996. ATRX encodes a novel member of the SNF2 family of proteins: mutations point to a common mechanism underlying the ATR-X syndrome. Hum. Mol. Genet. **5:**1899–1907. http://dx.doi.org/10.1093/hmg/5.12.1899.
20. **Baumann C, Viveiros MM, De La Fuente R.** 2010. Loss of maternal ATRX results in centromere instability and aneuploidy in the mammalian oocyte and preimplantation embryo. PLoS Genet. **6:**e1001137. http://dx.doi.org/10.1371/journal.pgen.1001137.
21. **Kernohan KD, Jiang Y, Tremblay DC, Bonvissuto AC, Eubanks JH, Mann MR, Berube NG.** 2010. ATRX partners with cohesin and MeCP2 and contributes to developmental silencing of imprinted genes in the brain. Dev. Cell **18:**191–202. http://dx.doi.org/10.1016/j.devcel.2009.12.017.
22. **Lewis PW, Elsaesser SJ, Noh KM, Stadler SC, Allis CD.** 2010. Daxx is an H3.3-specific histone chaperone and cooperates with ATRX in replication-independent chromatin assembly at telomeres. Proc. Natl. Acad. Sci. U. S. A. **107:**14075–14080. http://dx.doi.org/10.1073/pnas.1008850107.
23. **Xue Y, Gibbons R, Yan Z, Yang D, McDowell TL, Sechi S, Qin J, Zhou S, Higgs D, Wang W.** 2003. The ATRX syndrome protein forms a chromatin-remodeling complex with Daxx and localizes in promyelocytic leukemia nuclear bodies. Proc. Natl. Acad. Sci. U. S. A. **100:**10635–10640. http://dx.doi.org/10.1073/pnas.1937626100.
24. **Loyola A, Almouzni G.** 2007. Marking histone H3 variants: how, when and why? Trends Biochem. Sci. **32:**425–433. http://dx.doi.org/10.1016/j.tibs.2007.08.004.
25. **Ahmad K, Henikoff S.** 2002. The histone variant H3.3 marks active chromatin by replication-independent nucleosome assembly. Mol. Cell **9:**1191–1200. http://dx.doi.org/10.1016/S1097-2765(02)00542-7.
26. **Goldberg AD, Banaszynski LA, Noh KM, Lewis PW, Elsaesser SJ, Stadler S, Dewell S, Law M, Guo X, Li X, Wen D, Chapgier A, DeKelver RC, Miller JC, Lee YL, Boydston EA, Holmes MC, Gregory PD, Greally JM, Rafii S, Yang C, Scambler PJ, Garrick D, Gibbons RJ, Higgs DR, Cristea IM, Urnov FD, Zheng D, Allis CD.** 2010. Distinct factors control histone variant H3.3 localization at specific genomic regions. Cell **140:**678–691. http://dx.doi.org/10.1016/j.cell.2010.01.003.
27. **Negorev DG, Vladimirova OV, Ivanov A, Rauscher F, III, Maul GG.** 2006. Differential role of Sp100 isoforms in interferon-mediated repression of herpes simplex virus type 1 immediate-early protein expression. J. Virol. **80:**8019–8029. http://dx.doi.org/10.1128/JVI.02164-05.
28. **Woodhall DL, Groves IJ, Reeves MB, Wilkinson G, Sinclair JH.** 2006. Human Daxx-mediated repression of human cytomegalovirus gene expression correlates with a repressive chromatin structure around the major immediate-early promoter. J. Biol. Chem. **281:**37652–37660. http://dx.doi.org/10.1074/jbc.M604273200.
29. **Schreiner S, Burck C, Glass M, Groitl P, Wimmer P, Kinkley S, Mund A, Everett RD, Dobner T.** 2013. Control of human adenovirus type 5 gene expression by cellular Daxx/ATRX chromatin-associated complexes. Nucleic Acids Res. **41:**3532–3550. http://dx.doi.org/10.1093/nar/gkt064.
30. **Thorley-Lawson DA, Allday MJ.** 2008. The curious case of the tumour virus: 50 years of Burkitt's lymphoma. Nat. Rev. Microbiol. **6:**913–924. http://dx.doi.org/10.1038/nrmicro2015.
31. **Young LS, Rickinson AB.** 2004. Epstein-Barr virus: 40 years on. Nat. Rev. Cancer **4:**757–768. http://dx.doi.org/10.1038/nrc1452.
32. **Lieberman PM.** 2013. Keeping it quiet: chromatin control of gammaherpesvirus latency. Nat. Rev. Microbiol. **11:**863–875. http://dx.doi.org/10.1038/nrmicro3135.
33. **Lieberman PM.** 2006. Chromatin regulation of virus infection. Trends Microbiol. **14:**132–140. http://dx.doi.org/10.1016/j.tim.2006.01.001.
34. **Kalla M, Hammerschmidt W.** 2012. Human B cells on their route to latent infection-early but transient expression of lytic genes of Epstein-Barr virus. Eur. J. Cell Biol. **91:**65–69. http://dx.doi.org/10.1016/j.ejcb.2011.01.014.
35. **Johannsen E, Luftig M, Chase MR, Weicksel S, Cahir-McFarland E, Illanes D, Sarracino D, Kieff E.** 2004. Proteins of purified Epstein-Barr virus. Proc. Natl. Acad. Sci. U. S. A. **101:**16286–16291. http://dx.doi.org/10.1073/pnas.0407320101.
36. **Full F, Jungnickl D, Reuter N, Bogner E, Brulois K, Scholz B, Sturzl M, Myoung J, Jung JU, Stamminger T, Ensser A.** 2014. Kaposi's sarcoma

associated herpesvirus tegument protein ORF75 is essential for viral lytic replication and plays a critical role in the antagonization of ND10-instituted intrinsic immunity. PLoS Pathog. **10:**e1003863. http://dx.doi.org/10.1371/journal.ppat.1003863.

37. **Ling PD, Tan J, Sewatanon J, Peng R.** 2008. Murine gammaherpesvirus 68 open reading frame 75c tegument protein induces the degradation of PML and is essential for production of infectious virus. J. Virol. **82:**8000–8012. http://dx.doi.org/10.1128/JVI.02752-07.
38. **Full F, Reuter N, Zielke K, Stamminger T, Ensser A.** 2012. Herpesvirus saimiri antagonizes nuclear domain 10-instituted intrinsic immunity via an ORF3-mediated selective degradation of cellular protein Sp100. J. Virol. **86:**3541–3553. http://dx.doi.org/10.1128/JVI.06992-11.
39. **Feederle R, Neuhierl B, Baldwin G, Bannert H, Hub B, Mautner J, Behrends U, Delecluse HJ.** 2006. Epstein-Barr virus BNRF1 protein allows efficient transfer from the endosomal compartment to the nucleus of primary B lymphocytes. J. Virol. **80:**9435–9443. http://dx.doi.org/10.1128/JVI.00473-06.
40. **Tsai K, Thikmyanova N, Wojcechowskyj JA, Delecluse HJ, Lieberman PM.** 2011. EBV tegument protein BNRF1 disrupts DAXX-ATRX to activate viral early gene transcription. PLoS Pathog. **7:**e1002376. http://dx.doi.org/10.1371/journal.ppat.1002376.
41. **Lin DY, Shih HM.** 2002. Essential role of the 58-kDa microspherule protein in the modulation of Daxx-dependent transcriptional repression as revealed by nucleolar sequestration. J. Biol. Chem. **277:**25446–25456. http://dx.doi.org/10.1074/jbc.M200633200.
42. **Elsasser SJ, Huang H, Lewis PW, Chin JW, Allis CD, Patel DJ.** 2012. DAXX envelops a histone H3.3-H4 dimer for H3.3-specific recognition. Nature **491:**560–565. http://dx.doi.org/10.1038/nature11608.
43. **Conn KL, Hendzel MJ, Schang LM.** 2011. Core histones H2B and H4 are mobilized during infection with herpes simplex virus 1. J. Virol. **85:**13234–13252. http://dx.doi.org/10.1128/JVI.06038-11.
44. **Conn KL, Hendzel MJ, Schang LM.** 2013. The differential mobilization of histones H3.1 and H3.3 by herpes simplex virus 1 relates histone dynamics to the assembly of viral chromatin. PLoS Pathog. **9:**e1003695. http://dx.doi.org/10.1371/journal.ppat.1003695.
45. **Delecluse HJ, Hilsendegen T, Pich D, Zeidler R, Hammerschmidt W.** 1998. Propagation and recovery of intact, infectious Epstein-Barr virus from prokaryotic to human cells. Proc. Natl. Acad. Sci. U. S. A. **95:**8245–8250. http://dx.doi.org/10.1073/pnas.95.14.8245.
46. **Greenfield EA.** 2014. Antibodies: a laboratory manual, 2nd ed. Cold Spring Harbor Laboratory Press, Cold Spring Harbor, NY.
47. **Dignam JD, Lebovitz RM, Roeder RG.** 1983. Accurate transcription initiation by RNA polymerase II in a soluble extract from isolated mammalian nuclei. Nucleic Acids Res. **11:**1475–1489. http://dx.doi.org/10.1093/nar/11.5.1475.
48. **Luger K, Rechsteiner TJ, Richmond TJ.** 1999. Preparation of nucleosome core particle from recombinant histones. Methods Enzymol. **304:**3–19. http://dx.doi.org/10.1016/S0076-6879(99)04003-3.
49. **Conn KL, Hendzel MJ, Schang LM.** 2008. Linker histones are mobilized during infection with herpes simplex virus type 1. J. Virol. **82:**8629–8646. http://dx.doi.org/10.1128/JVI.00616-08.
50. **Tempera I, Wiedmer A, Dheekollu J, Lieberman PM.** 2010. CTCF prevents the epigenetic drift of EBV latency promoter Qp. PLoS Pathog. **6:**e1001048. http://dx.doi.org/10.1371/journal.ppat.1001048.
51. **Law MJ, Lower KM, Voon HP, Hughes JR, Garrick D, Viprakasit V, Mitson M, De Gobbi M, Marra M, Morris A, Abbott A, Wilder SP, Taylor S, Santos GM, Cross J, Ayyub H, Jones S, Ragoussis J, Rhodes D, Dunham I, Higgs DR, Gibbons RJ.** 2010. ATR-X syndrome protein targets tandem repeats and influences allele-specific expression in a size-dependent manner. Cell **143:**367–378. http://dx.doi.org/10.1016/j.cell.2010.09.023.
52. **Dheekollu J, Wiedmer A, Hayden J, Speicher D, Gotter AL, Yen T, Lieberman PM.** 2011. Timeless links replication termination to mitotic kinase activation. PLoS One **6:**e19596. http://dx.doi.org/10.1371/journal.pone.0019596.
53. **Chen HS, Martin KA, Lu F, Lupey LN, Mueller JM, Lieberman PM, Tempera I.** 2014. Epigenetic deregulation of the LMP1/LMP2 locus of Epstein-Barr virus by mutation of a single CTCF-cohesin binding site. J. Virol. **88:**1703–1713. http://dx.doi.org/10.1128/JVI.02209-13.
54. **Anand R, Hoskins AA, Stubbe J, Ealick SE.** 2004. Domain organization of *Salmonella typhimurium* formylglycinamide ribonucleotide amidotransferase revealed by X-ray crystallography. Biochemistry **43:**10328–10342. http://dx.doi.org/10.1021/bi0491301.
55. **Kimura H.** 2005. Histone dynamics in living cells revealed by photobleaching. DNA Repair **4:**939–950. http://dx.doi.org/10.1016/j.dnarep.2005.04.012.
56. **Lukashchuk V, Everett RD.** 2010. Regulation of ICP0-null mutant herpes simplex virus type 1 infection by ND10 components ATRX and hDaxx. J. Virol. **84:**4026–4040. http://dx.doi.org/10.1128/JVI.02597-09.
57. **Lukashchuk V, McFarlane S, Everett RD, Preston CM.** 2008. Human cytomegalovirus protein pp71 displaces the chromatin-associated factor ATRX from nuclear domain 10 at early stages of infection. J. Virol. **82:**12543–12554. http://dx.doi.org/10.1128/JVI.01215-08.
58. **Newhart A, Rafalska-Metcalf IU, Yang T, Negorev DG, Janicki SM.** 2012. Single-cell analysis of Daxx- and ATRX-dependent transcriptional repression. J. Cell Sci. **125:**5489–5501. http://dx.doi.org/10.1242/jcs.110148.
59. **Shannon-Lowe C, Adland E, Bell AI, Delecluse HJ, Rickinson AB, Rowe M.** 2009. Features distinguishing Epstein-Barr virus infections of epithelial cells and B cells: viral genome expression, genome maintenance, and genome amplification. J. Virol. **83:**7749–7760. http://dx.doi.org/10.1128/JVI.00108-09.
60. **Ishov AM, Vladimirova OV, Maul GG.** 2004. Heterochromatin and ND10 are cell-cycle regulated and phosphorylation-dependent alternate nuclear sites of the transcription repressor Daxx and SWI/SNF protein ATRX. J. Cell Sci. **117:**3807–3820. http://dx.doi.org/10.1242/jcs.01230.
61. **Tierney R, Kirby H, Nagra J, Rickinson A, Bell A.** 2000. The Epstein-Barr virus promoter initiating B-cell transformation is activated by RFX proteins and the B-cell-specific activator protein BSAP/Pax5. J. Virol. **74:**10458–10467. http://dx.doi.org/10.1128/JVI.74.22.10458-10467.2000.
62. **Jiao Y, Shi C, Edil BH, de Wilde RF, Klimstra DS, Maitra A, Schulick RD, Tang LH, Wolfgang CL, Choti MA, Velculescu VE, Diaz LA, Jr, Vogelstein B, Kinzler KW, Hruban RH, Papadopoulos N.** 2011. DAXX/ATRX, MEN1, and mTOR pathway genes are frequently altered in pancreatic neuroendocrine tumors. Science **331:**1199–1203. http://dx.doi.org/10.1126/science.1200609.
63. **Schwartzentruber J, Korshunov A, Liu XY, Jones DT, Pfaff E, Jacob K, Sturm D, Fontebasso AM, Quang DA, Tonjes M, Hovestadt V, Albrecht S, Kool M, Nantel A, Konermann C, Lindroth A, Jager N, Rausch T, Ryzhova M, Korbel JO, Hielscher T, Hauser P, Garami M, Klekner A, Bognar L, Ebinger M, Schuhmann MU, Scheurlen W, Pekrun A, Fruhwald MC, Roggendorf W, Kramm C, Durken M, Atkinson J, Lepage P, Montpetit A, Zakrzewska M, Zakrzewski K, Liberski PP, Dong Z, Siegel P, Kulozik AE, Zapatka M, Guha A, Malkin D, Felsberg J, Reifenberger G, von Deimling A, Ichimura K, Collins VP, Witt H, Milde T, Witt O, Zhang C, Castelo-Branco P, Lichter P, Faury D, Tabori U, Plass C, Majewski J, Pfister SM, Jabado N.** 2012. Driver mutations in histone H3.3 and chromatin remodeling genes in paediatric glioblastoma. Nature **482:**226–231. http://dx.doi.org/10.1038/nature10833.
64. **Heaphy CM, de Wilde RF, Jiao Y, Klein AP, Edil BH, Shi C, Bettegowda C, Rodriguez FJ, Eberhart CG, Hebbar S, Offerhaus GJ, McLendon R, Rasheed BA, He Y, Yan H, Bigner DD, Oba-Shinjo SM, Marie SK, Riggins GJ, Kinzler KW, Vogelstein B, Hruban RH, Maitra A, Papadopoulos N, Meeker AK.** 2011. Altered telomeres in tumors with ATRX and DAXX mutations. Science **333:**425. http://dx.doi.org/10.1126/science.1207313.
65. **Drane P, Ouararhni K, Depaux A, Shuaib M, Hamiche A.** 2010. The death-associated protein DAXX is a novel histone chaperone involved in the replication-independent deposition of H3.3. Genes Dev. **24:**1253–1265. http://dx.doi.org/10.1101/gad.566910.
66. **Clynes D, Higgs DR, Gibbons RJ.** 2013. The chromatin remodeler ATRX: a repeat offender in human disease. Trends Biochem. Sci. **38:**461–466. http://dx.doi.org/10.1016/j.tibs.2013.06.011.
67. **Gibson W, Roizman B.** 1971. Compartmentalization of spermine and spermidine in the herpes simplex virion. Proc. Natl. Acad. Sci. U. S. A. **68:**2818–2821. http://dx.doi.org/10.1073/pnas.68.11.2818.
68. **Placek BJ, Huang J, Kent JR, Dorsey J, Rice L, Fraser NW, Berger SL.** 2009. The histone variant H3.3 regulates gene expression during lytic infection with herpes simplex virus type 1. J. Virol. **83:**1416–1421. http://dx.doi.org/10.1128/JVI.01276-08.
69. **Penkert RR, Kalejta RF.** 2011. Tegument protein control of latent herpesvirus establishment and animation. Herpesviridae **2:**3. http://dx.doi.org/10.1186/2042-4280-2-3.
70. **Saffert RT, Kalejta RF.** 2007. Human cytomegalovirus gene expression is silenced by Daxx-mediated intrinsic immune defense in model latent infections established in vitro. J. Virol. **81:**9109–9120. http://dx.doi.org/10.1128/JVI.00827-07.